

The first few months of a supernova remnant

Michael Gabler¹, Annop Wongwathanarat², Hans-Thomas Janka¹, Ewald Müller¹

¹ Max-Planck-Institut für Astrophysik, Garching (Germany); ² RIKEN, Wako (Japan)

Motivation

- While first neutrino-driven supernova explosions have been obtained recently in 3D, self-consistent, first-principle simulations, these models are still not exploding robustly and, in general, the explosions are not sufficiently energetic. The deficits of the simulations could be associated with numerical issues (resolution), progenitor properties (rotation, magnetic fields or pre-collapse perturbations), or with microphysics (more efficient neutrino heating)
- To constrain the explosion mechanism it is thus very helpful to consider other observational constraints: pulsar kicks, progenitor association and supernova remnants (SNR). The observation of asymmetries in the supernova ejecta (high ratio of Ti44/Ni56 emission, optical light echoes, jet-like features in the X-ray and optical ejecta, and spatially resolved X-ray emission (Fig.1)) is very promising, since the long-term simulations of the explosion have to provide comparable structures.

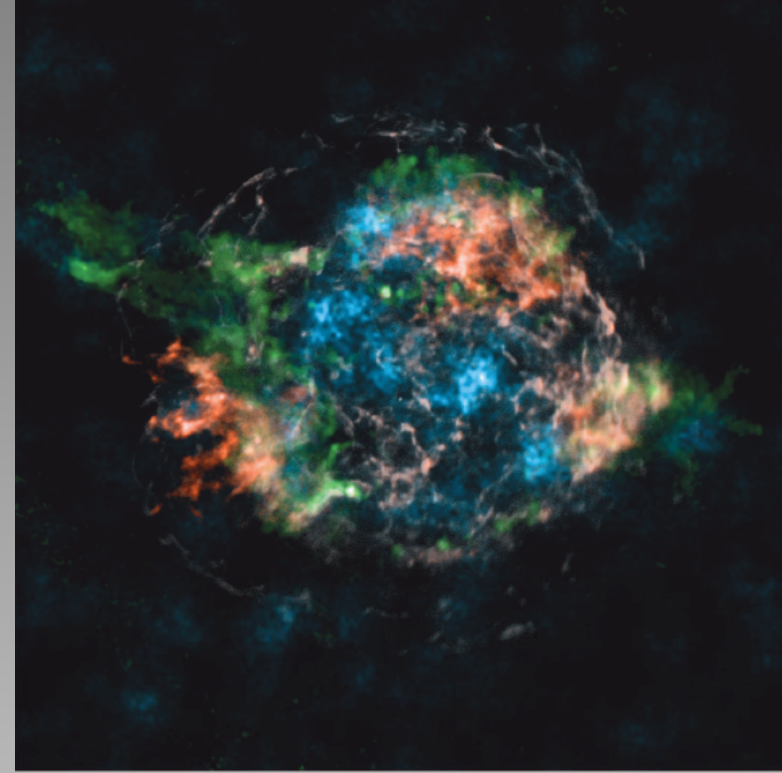


Fig.1 Grefenstette et al. (2015): Spatial distribution of Ti44 (blue), Si/Mg (green) and Fe (red)

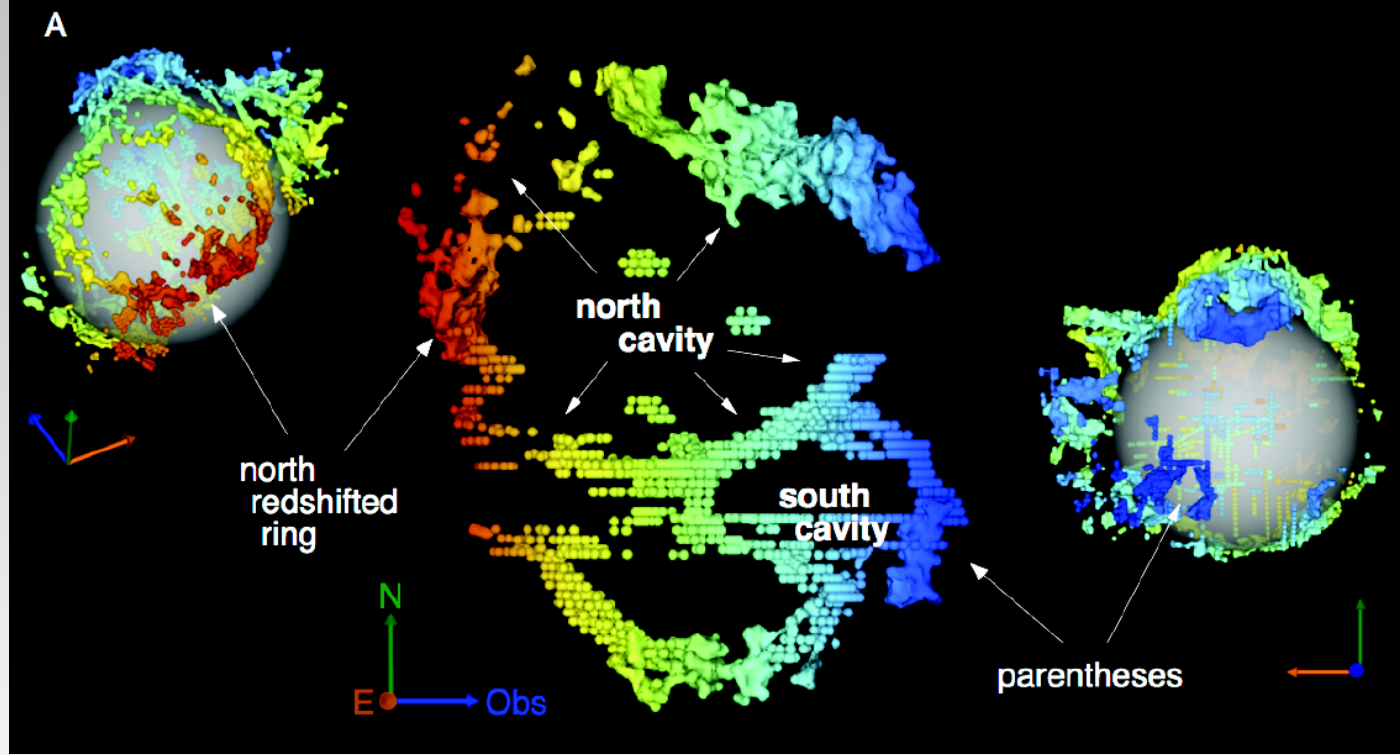


Fig.2 Milisavljevic & Fesen (2015): Doppler reconstruction of Cas A from the [S III] emission

- First spatial maps and spectral properties of radioactively decaying Ti44 show large asymmetries (Fig.1). The lack of correlation between Ti44 emission and observed Fe may be due to the hidden, unshocked and non-radiating Fe in the regions of high Ti44 concentrations
- Near-infrared observations of Cassiopeia A, allow for a three-dimensional map of its interior, unshocked ejecta (Fig.2) and show a bubble-like morphology. This ejecta structure may have been originated from plumes caused by hydrodynamical instabilities during the explosion that later got inflated by additional energy input due to Ni-decay.

The model

- We continue three-dimensional hydrodynamical simulations of core-collapse supernovae for four stellar models (see Table 1). The initial simulations finished shortly after the shock breakout from the surface of the progenitor star.
- For the simulations we use the Prometheus code an explicit, finite-volume Eulerian multi-fluid hydrodynamic code which uses dimensional splitting, PPM reconstruction, the consistent multifluid advection scheme and the AUSM+ fluxes. Instead of the usual spherical polar grid, the code uses the axis free "Yin-Yang" overlapping grid technique that prevents from numerical problems at the symmetry axis and allows for a more generous CFL condition.
- For densities above 10^{-10} g/cm³, temperatures above 10^4 K we use a tabulated equation of state that includes arbitrarily degenerate and relativistic electrons and positrons, Planckian photons and a set of nuclei treated as a mixture of ideal gases. Below the threshold there should be no free positrons and the electrons are treated as an ideal gas too. Once the matter becomes transparent to photons, the EOS does no longer consider the photon contribution and the latter leave the system taking their energy away with them.
- The most important radioactive element is Ni56. It decays like: Ni56 ($\tau_{1/2} \sim 6d$) \rightarrow Co56 ($\tau_{1/2} \sim 77d$) \rightarrow Fe56. The total energy budget for these two transitions is $E_{\text{radioactive}} \sim 10^{49}$ erg ($\ll E_{\text{exp}} \sim 10^{51}$ erg). Part of this energy can increase the internal energy, which then will be used to isotropically expand the heated material, or, when the matter becomes transparent at later times, the other part can escape in the form of photons and power the light curve.

Model	Type	Mass [M_{\odot}]	R_{*} [10^6 km]	E_{exp} [B]
W15	RSG	15	339	1.13
L15	RSG	15	434	1.13
N20	BSG	20	33.8	1.35
B15	BSG	15	39	1.25

Table 1: Properties of the stellar progenitor models. We used two blue supergiants (BSG) and two red supergiants (RSG).

Ni rich ejecta of model B15

- Strong Rayleigh-Taylor (RT) instabilities develop at the shell interfaces of the progenitor. The large initial plumes (first panel) of the explosion fragment into many RT fingers (second panel).
- At the outbreak, the velocity at the top of the RT fingers is larger than at the center and the fingers grow further preserving the very fine structures (third panel).
- The energy input caused by the radioactively decaying Ni56 and Co56 leads to an inflation of the RT fingers (fourth panel).

Ni rich ejecta of model N20

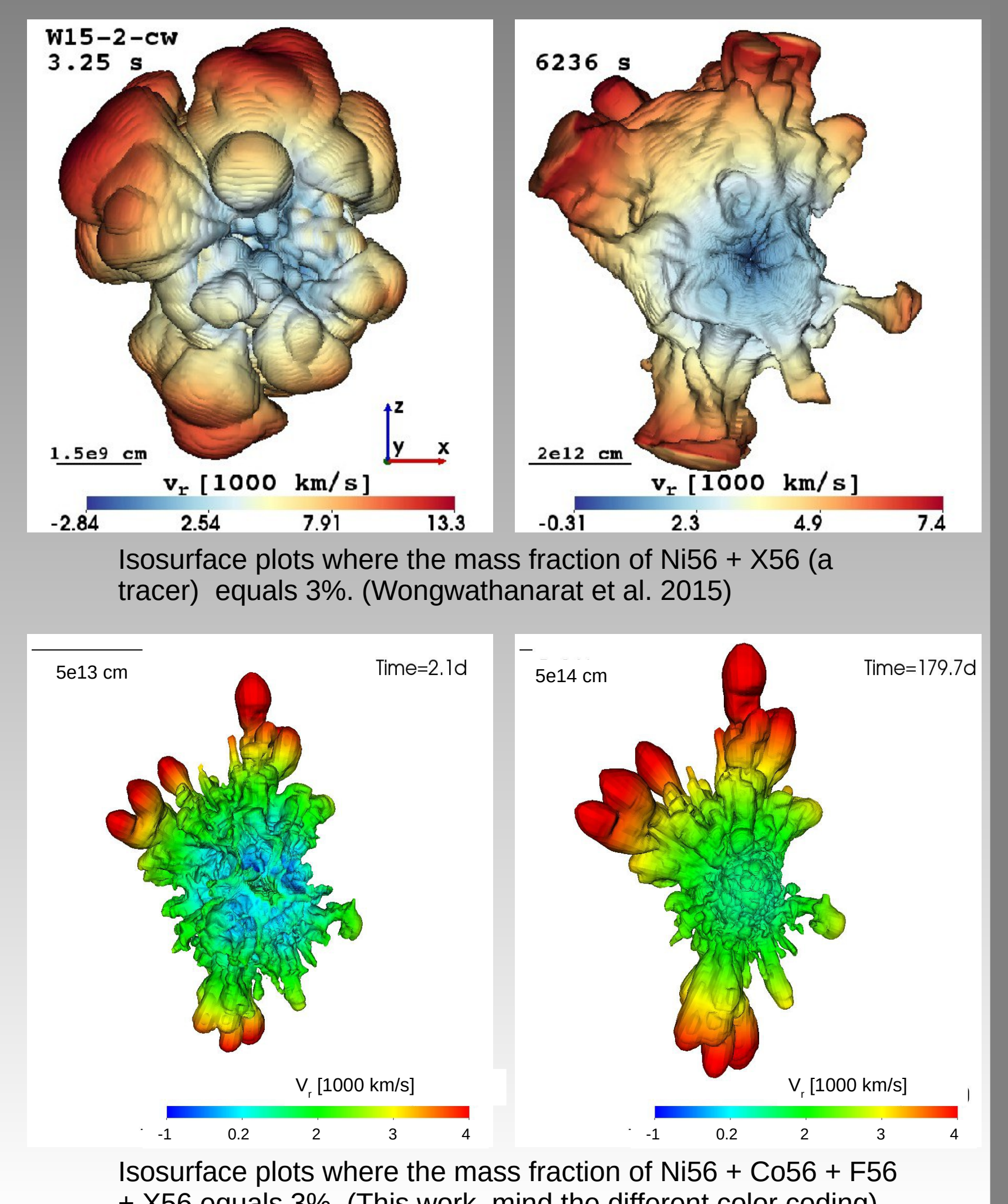
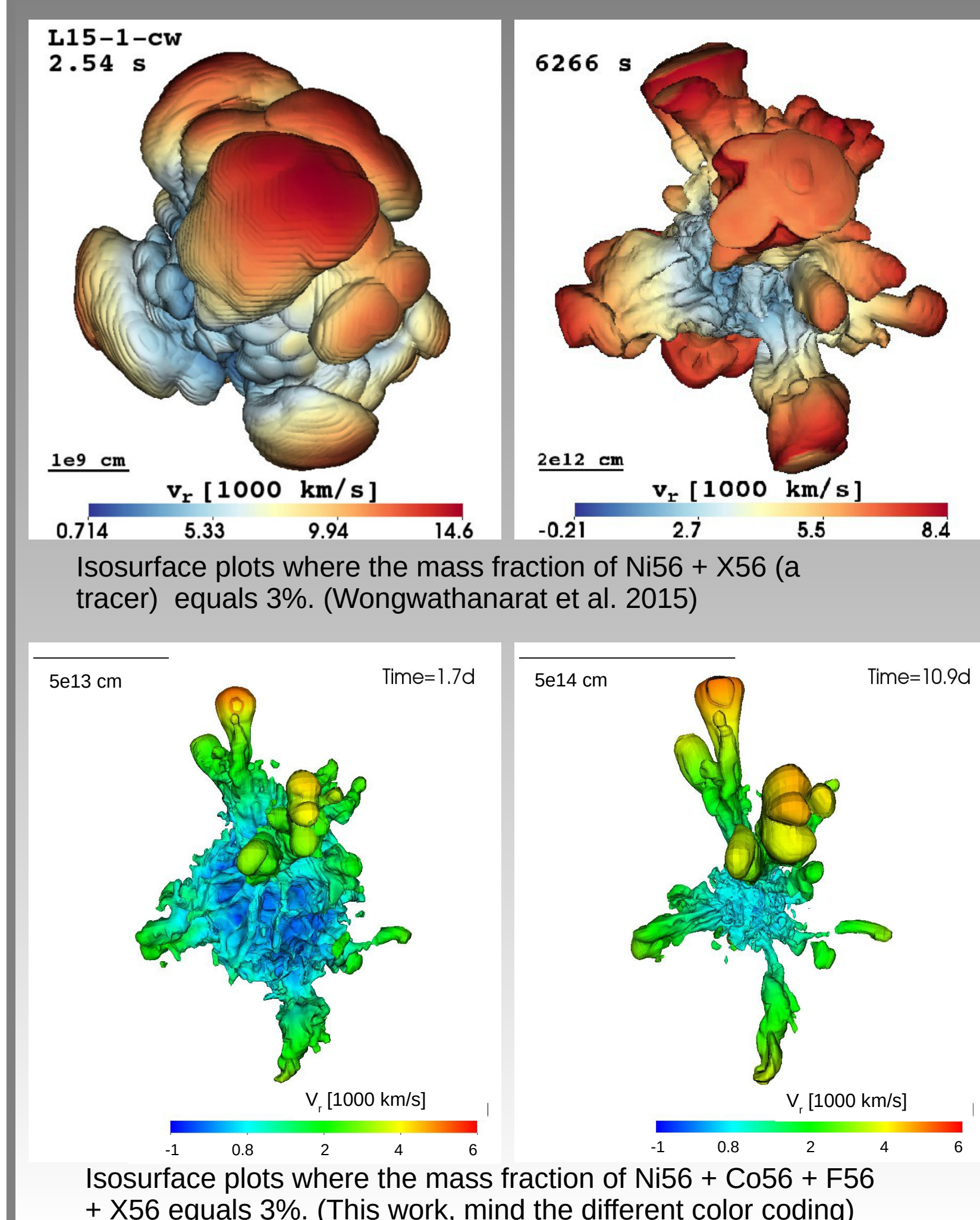
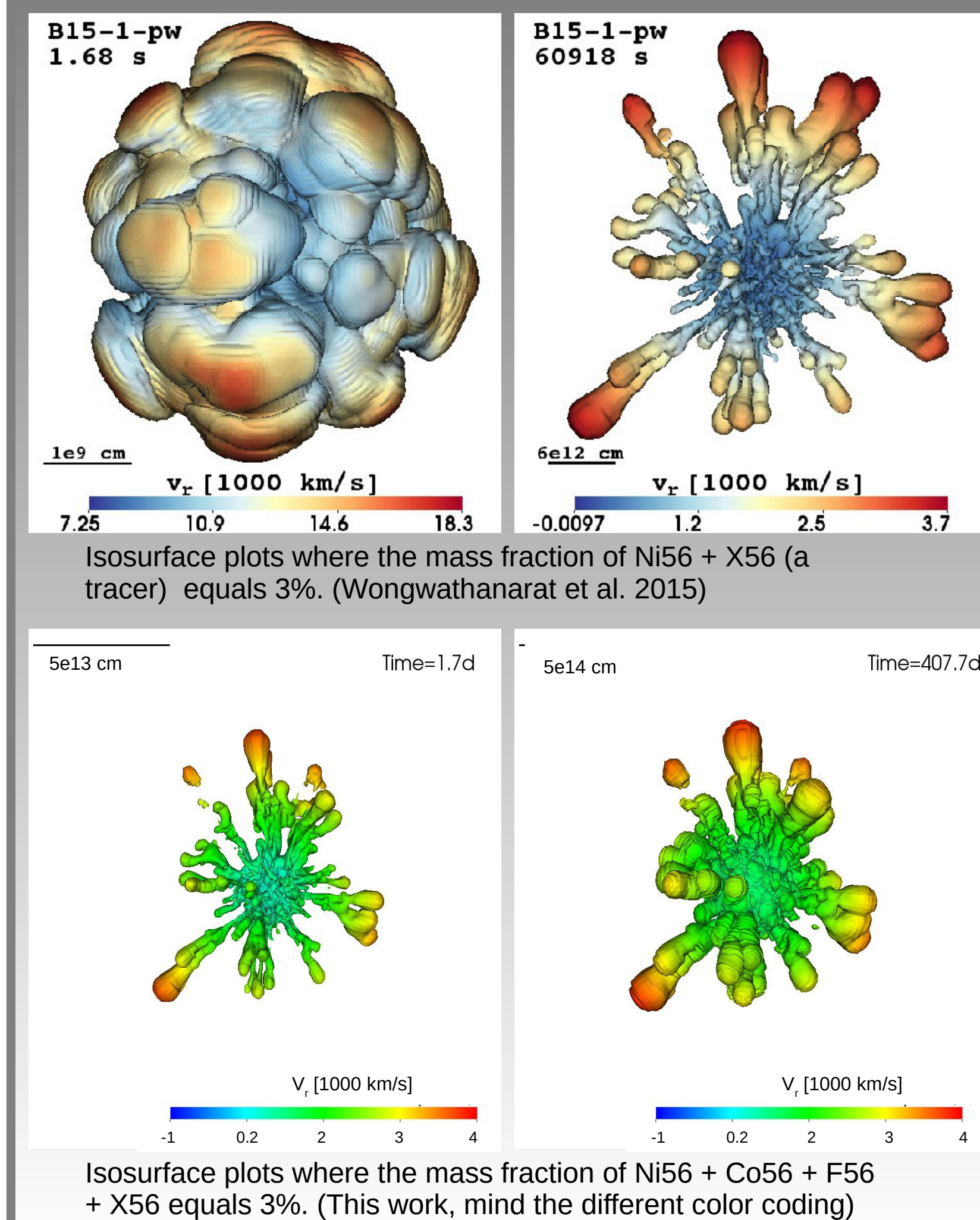
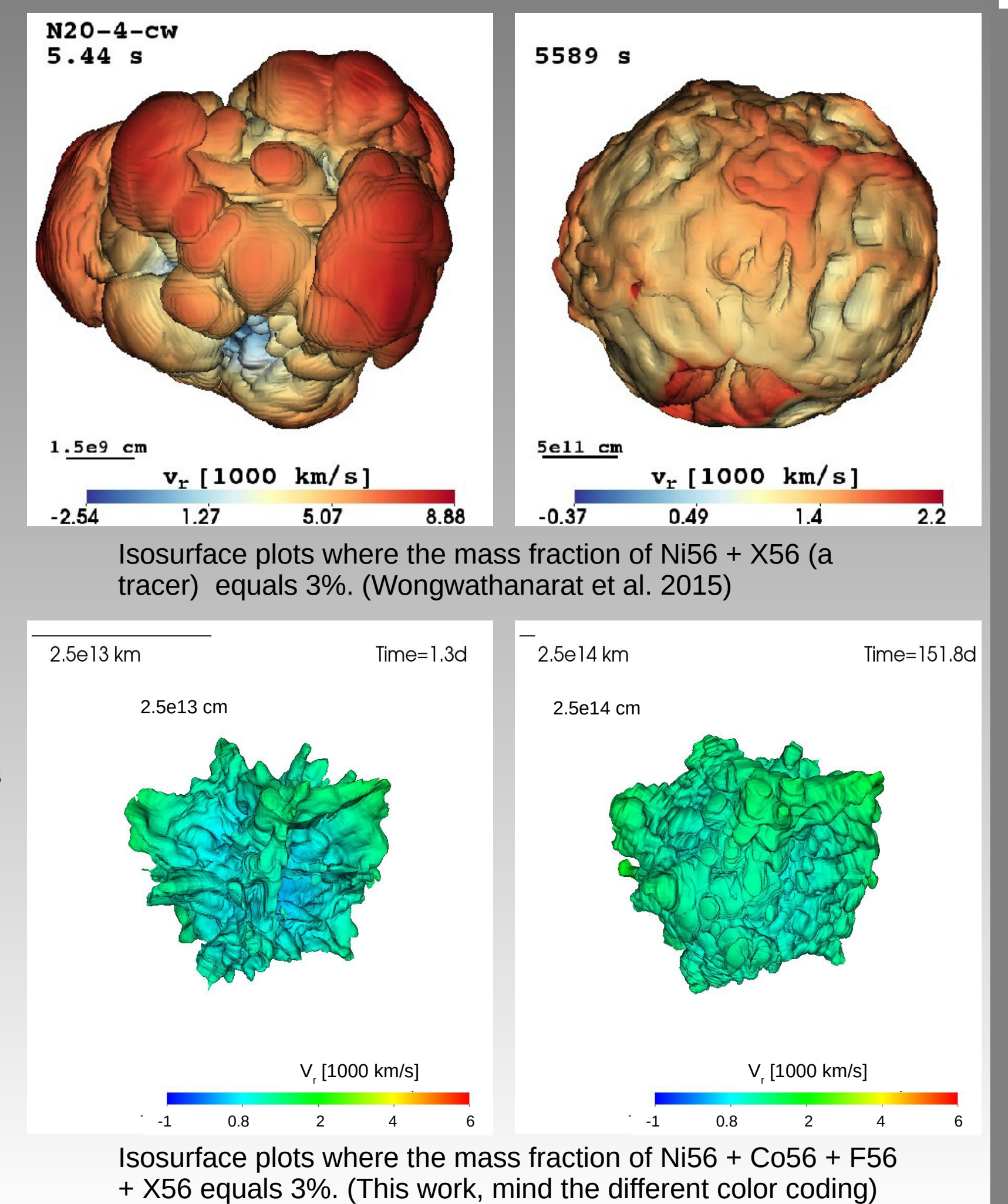
- The large initial plumes (first panel) of the explosion stay almost unchanged inside the progenitor, because there is no time for RT instability to operate.
- The plumes get compressed significantly by the reverse shock forming at the He/H-interface and the ejecta become almost spherical (second panel).
- After the outbreak, velocity differences lead to increasing asymmetries (third plot).
- The energy input caused by the radioactively decaying Ni56 and Co56 inflates the Ni-rich structures which smears out the asymmetries and makes the ejecta more spherical again.

Ni rich ejecta of model L15

- The initial plumes (first panel) show a high degree of asymmetry originating from the explosion dynamics.
- When propagating through the progenitor these plumes are not as drastically fragmented by the RT-instability and the reverse shock compressed the top of the RT-fingers towards the center of the explosion (second panel).
- After the outbreak, existing plumes/fingers grow further creating finer structures (third panel).
- The energy input from beta decay inflates the structures again (fourth panel, mind the very short time of only 10d for this simulation which did not allow for significant energy input yet).

Ni rich ejecta of model W15

- The asymmetry in the big plumes (first panel) are the fingerprint of the explosion dynamics.
- Some RT fingers develop during the propagation through the progenitor, however, they are compressed by the reverse shock (second panel).
- After the outbreak the compressed RT-fingers fragment further and grow significantly (panel three).
- Finally the inflation of the RT-fingers due to the energy input from the beta decay leads to the merging of neighbouring structures.



Conclusions:

- Imprints of the initial asymmetries are carried through the evolution until late stages. The final structures can still be associated with large-scale plumes that are created during the explosion and carry the imprint of hydrodynamical instabilities of the explosion mechanism.
- The large-scale plumes get fragmented due to Rayleigh-Taylor instabilities that can grow at shell interfaces of the progenitor. Therefore, the progenitor structure determines the strength of the fragmentation: The model N20 shows very little fragmentation while B15 or W15 show very strong fragmentation.
- After the outbreak from the progenitor surface, the fragmented plumes start to grow in size due to the additional energy input coming from the radioactive decay of Ni56. Some of the Rayleigh-Taylor fingers merge and create larger structures. The ejecta have not yet reached their final structure, however we do not expect further significant changes to our late time models. The simulations are currently continued to later times.

Bibliography

- DeLaney et al., ApJ, 725, 20138 (2010)
 Fesen et al., ApJ, 645, 283 (2006)
 Fesen & Milisavljevic, ApJ, 818, 19 (2016)
 Grefenstette et al., Nature, 506 339 (2014)
 Hammer et al., ApJ, 714, 1371 (2010)
 Herant & Benz, ApJ, 370, L81 (1991)
- Hwang et al., ApJ, 615, L117 (2004)
 Kifonidis et al., ApJ, 531, L123 (2000)
 Kifonidis et al., A&A, 453, 661 (2006)
 Milisavljevic & Fesen, ApJ, 772, 15 (2013)
 Milisavljevic & Fesen, Science, 347, 526 (2015)
 Nagataki et al., ApJ, 492, L45 (1998)

- Rest et al., ApJ, 732, 3 (2011)
 Utrobin et al. A&A, 581, 18 (2015)
 Wongwathanarat et al., A&A, 514, 14 (2010)
 Wongwathanarat et al., ApJL, 725, L106 (2010)
 Wongwathanarat et al., A&A, 552, 25 (2013)
 Wongwathanarat et al., A&A, 577, 20 (2015)